

ORIGINAL RESEARCH

OPEN ACCESS



## Tertiary lymphoid structures and their association to immune phenotypes and circulatory IL2 levels in pancreatic ductal adenocarcinoma

Azaz Ahmed<sup>a,b</sup>, Sophia Köhler<sup>a</sup>, Rosa Klotz<sup>c</sup>, Nathalia Giese<sup>c</sup>, Thilo Hackert<sup>c</sup>, Christoph Springfeld<sup>a</sup>, Inka Zörnig<sup>a</sup>, Dirk Jäger<sup>a,d</sup>, and Niels Halama<sup>a,b</sup>

<sup>a</sup>Medical Oncology and Internal Medicine VI, National Center for Tumor Diseases (NCT), University Hospital Heidelberg, University Heidelberg, Heidelberg, Germany; <sup>b</sup>Translational Immunotherapy (D240), German Cancer Research Center (DKFZ), Heidelberg, Germany; <sup>c</sup>General, Visceral and Transplantation Surgery, University Hospital Heidelberg, University Heidelberg, Heidelberg, Germany; <sup>d</sup>Applied Tumor Immunity Clinical Cooperation Unit (D120), National Center for Tumor Diseases (NCT), German Cancer Research Center (DKFZ), Heidelberg, Germany

### ABSTRACT

Pancreatic ductal adenocarcinoma (PDA) is usually unresponsive to immunotherapeutic approaches. However, tertiary lymphoid structures (TLS) are associated with favorable patient outcomes in PDA. A better understanding of the B cell infiltrate and biological features of TLS formation is needed to further explore their potential and improve patient management. We analyzed tumor tissues (n = 55) and corresponding blood samples (n = 51) from PDA patients by systematic immunohistochemistry and multiplex cytokine measurements. The tissue was compartmentalized in “tumor” and “stroma” and separately examined. Clinical patient information was used to perform survival analyses. We found that the mere number of B cells is not associated with patient survival, but formation of TLS in the peritumoral stroma is a prognostic favorable marker in PDA patients. TLS-positive tissues show a higher density of CD8<sup>+</sup> T cells and CD20<sup>+</sup> B cells and a higher IL2 level in the peritumoral stroma than tissues without TLS. Compartmental assessment shows that gradients of IL2 expression differ with regard to TLS formation: TLS presence is associated with higher IL2 levels in the stromal than in the tumoral compartment, while no difference is seen in patients without TLS. Focusing on the stroma-to-serum gradient, only patients without TLS show significantly higher IL2 levels in the serum than in stroma. Finally, low circulatory IL2 levels are associated with local TLS formation. Our findings highlight that TLS are prognostic favorable and associated with antitumoral features in the microenvironment of PDA. Also, we propose easily accessible serum IL2 levels as a potential marker for TLS prediction.

### ARTICLE HISTORY

Received 6 October 2021  
Revised 17 December 2021  
Accepted 17 December 2021

### KEYWORDS

Tertiary lymphoid structures;  
Pancreatic ductal  
adenocarcinoma;  
Interleukin-2

## Introduction

The immunological characterization of the tumor microenvironment (TME) is a key aspect to improving patient outcomes in various cancer entities. The development and progression of pancreatic ductal adenocarcinoma (PDA) is closely linked to local and systemic immune responses. The pancreatic TME is characterized by a desmoplastic stroma with increased extracellular matrix and collagen, enrichment of immunosuppressor cells like FoxP3<sup>+</sup> regulatory T cells and tumor-supportive CD163<sup>+</sup> M2 macrophages and scarcity of CD8<sup>+</sup> effector T cells.<sup>1</sup> All these aspects contribute to the dismal prognosis of PDA patients. However, while the presence of B cells is common in PDA, their role in disease remains controversial. On the one hand, preclinical studies describe the involvement of B cells in supporting pancreatic tumorigenesis by suppression of other immune cells (e. g. CD8<sup>+</sup> T cells) and promoting pancreatic cancer cell proliferation.<sup>2–4</sup> On the other hand, clinical data indicate that B cells are a prognostic favorable factor for PDA patients.<sup>5,6</sup>

B cells in malignancies not only appear as scatteringly infiltrating immune cells but also organized within tertiary lymphoid structures (TLS). TLS are ectopic lymphoid aggregates mainly appearing at sites of chronic inflammation such as tumors.<sup>7</sup> Formation of TLS has been identified in a large variety of human cancers at all disease stages with high variability between tumor entities and patients.<sup>6</sup> Their grade of organization can vary from mere assembly of B and T cells with dendritic cells to lymphoid organs containing B and T cell zones, dendritic cells, lymphatic vessels and high endothelial venules. The presence of TLS positively correlates with clinical benefit in multiple tumor entities including PDA.<sup>5</sup> Further, it is considered that TLS actively enhance anti-tumor immunity, and they are supposed to promote response to immunotherapy (e. g. in metastatic melanoma and renal cell carcinoma).<sup>8</sup>

A compartmental investigation of the local and systemic immune landscape can expand our understanding of tumor immunity in PDA, especially with regard to B cell infiltration, including the formation of TLS. Besides, identification of easily

accessible serum biomarkers for TLS formation could improve clinical management strategies and help to translate relevant findings to the clinic by serving as a stratification tool.

In this study, we systematically analyzed human PDA tissues regarding their immune cell infiltration patterns and differential evaluation of compartmental cytokine gradients (stroma-to-tumor and stroma-to-serum) on a protein level. Our aim was to elucidate the role of B cells in PDA with focus on TLS formation and compartmentally decipher their impact on the tumor microenvironment and patient outcomes. Moreover, we intended to identify easily extractable circulatory markers associated with TLS formation.

## Materials and methods

### Patient cohort

Previously untreated PDA patients with preoperatively obtained serum samples, available frozen tumor tissue samples as well as available clinical baseline and outcome parameters were included. The prospectively maintained electronic pancreas database of the Department for General, Visceral and Transplantation Surgery at the University Hospital Heidelberg was searched for patients undergoing pancreatic surgery between 03/2007 and 07/2011. Tissue and data collection were approved by the local ethics committee of the University of Heidelberg (323/2004). Written informed consent was obtained from all patients.

### Data collection and outcome parameters

Baseline data were extracted from the database as follows: Gender, age, weight, body mass index and comorbidities (cardiovascular, pulmonary, renal, hepatic, autoimmune, diabetes). Preoperative serum values of carbohydrate antigen 19-9 were obtained from the hospital's laboratory information system. The overall survival in days was also assessed. Pathological reports included pTNM tumor stage according to the TNM Staging Manual, American Joint Committee on Cancer (AJCC), tumor grading and resection margin status.<sup>9</sup>

### Immunohistochemical staining

4  $\mu$ m tissue slices were prepared from cryopreserved tissue and mounted on glass slides. Immunohistochemistry was performed according to manufacturer's instructions using an automated staining facility (Bond Max, Leica, Germany). The following mouse monoclonal antibodies were used: CD3 $\epsilon$  (clone PS1, 1:100), CD20 (clone L26, 1:100), CD4 (clone 4B12, 1:150), CD8 (clone 4B11, 1:100), CD163 (clone EDHu-1, 1:500), CD21 (clone 2G9, 1:50). CD3 $\epsilon$ , CD20, CD4, CD8: Novocastra (Leica, Germany); CD163: Bio-Rad AbD Serotec (UK).

### Immune cell quantification

Immune cells were quantified using a software-based image analyzing system. Whole-slide images were acquired with NanoZoomer 2.0 HT scan system (Hamamatsu, Japan). All slides were scanned at 40x magnification. Cell density in immune cell

conglomerates was estimated as described before.<sup>10</sup> Further analysis was conducted using an image analysis software (VIS software suite, Visiopharm, Denmark). Quantification algorithms were applied individually for each distinctive staining protocol according to the strength of DAB staining.

### Protein quantification in stromal and tumor epithelial compartment

Cryopreserved PDA tissue samples were cut into multiple consecutive sections (20  $\mu$ m) and stained with cresyl-violet. Areas of tumor epithelium and stroma were highlighted at 20x magnification by brightfield-microscopy. Laser microdissection was performed with the Leica Laser Microdissection V5.0.2.0 software. Sufficient protein concentrations for Multiplex analysis could be won by dissection of 30–50  $\times$  106 mm<sup>2</sup>. Tissue was lysated using the BioPlex™ Cell Lysis Kit (Bio-Plex Cell Lysis Kit, BioRad, USA; 171304011) according to manufacturer's instructions. Serum samples were thawed overnight at 4°C and diluted 1:1 prior to protein quantification (Sample Diluent, BioRad, USA). A two-laser array reader simultaneously quantified all proteins of interest. The concentrations were calculated with Bio-Plex Manager 4.1.1 based on a 5-parameter logistic plot regression formula. Bio-Plex Pro Human Cytokine Screening Panel 48-plex (BioRad, USA; 12007283), Bio-Plex Pro Human Cytokine ICAM-1 (BioRad, USA; 171B6009M) and Bio-Plex Pro Human Cytokine VCAM-1 (BioRad, USA; 171B6022M) were used for cytokine quantification.

### Measurement of CA 19-9

Blood samples of the PDA patients were analyzed in the Core Laboratory Facilities of the University Hospital Heidelberg for the concentration of CA 19-9 (normal range <34 U/ml), according to accredited standards (DIN EN ISO 15189, D-ML-13060-01-00).

### Statistical analysis

Mann Whitney tests were used for non-paired samples. For paired samples, Wilcoxon matched-pairs signed rank tests were used. The latest information was used to assess the overall survival time. For survival analysis based on stromal B cell density, patients were stratified into two groups ("high" and "low") by determining the median cutpoints. For survival analysis based on the formation of TLS, patients were stratified into two groups ("TLS" and "No TLS") according to immunohistological formation of TLS. For survival analysis based on CD21 gene expression, we used gene expression data (TCGA Pancreatic Cancer) via the Xena platform.<sup>11</sup> Survival curves were visualized using the Kaplan–Meier estimators. Overall survival between patient groups was compared using the log-rank test. Differences were considered significant in the case of a p-value  $\leq$  and represented as follows: p  $\leq$  .05, \*\*p  $\leq$  .005 and \*\*\*p  $\leq$  .0001. All analyses were performed using the statistical software GraphPad Prism 8.4.1 software.

**Table 1.** Patient characteristics.

Characteristic	Subgroup		P-Value
	TLS (n = 17)	No TLS (n = 38)	
Female/Male (n/n)	9/8	19/19	> 0.99
Age (years)	68.21 ± 2.24	65.19 ± 1.73	
>/≤ Average age (n/n)	12/5	20/18	0.25
BMI <sup>a</sup>	24.12 ± 0.75	24.81 ± 0.67	
>/≤ Average BMI (n/n)	8/7	13/15	0.75
Diabetes mellitus (n)	7	12	0.55
Glucocorticoid or immunosuppressive drug intake (n)	0	2	> 0.99
Cardiovascular comorbidities (n)	10	19	0.57
Pulmonary comorbidities (n)	1	4	> 0.99
Renal comorbidities (n)	2	2	0.58
Hepatic comorbidities (n)	1	0	0.31
Autoimmune comorbidities (n)	0	2	> 0.99
T			
T3 (n)	17	37	> 0.99
T4 (n)	0	1	
N			
N0 (n)	4	6	0.48
N1 (n)	11	32	0.15
N2 (n)	2	0	0.09
M			
M0 (n)	16	36	> 0.99
M1 (n)	1	2	
Grade			
G2 (n)	13	23	0.36
G3 (n)	4	15	
R <sup>b</sup>			
R0 (n)	6	3	0.02
R1 (n)	11	34	

Data are shown as mean ± SEM. Fisher's exact test was used to compare patients of the different groups. BMI = body mass index (calculated as weight in kilograms divided by height in meters squared), T = stage of primary tumor, N = regional lymph node status, M = distant metastasis status, R = resection margin status.

<sup>a</sup>Information available on BMI status from 43 patients.

<sup>b</sup>Information available on resection margin status from 54 patients.

## Results

### Patients and baseline characteristics

We received serum and tumor tissue samples from 55 PDA patients who underwent pancreatic surgery between March 2007 and July 2011. As provided in Table 1, the cohort consisted of 28 men (50.9%) and 27 women (49.1%), with a mean age of 66.12 (± 1.38). In all patients, the histopathological diagnosis was PDA, with 54 patients (98.2%) having the tumor status pT3 and 1 patient (1.8%) with pT4. None of the patients received prior neoadjuvant chemotherapy. The only characteristic associated with TLS presence was the resection margin status of patients (Table 1).

### B cell infiltrate in PDA

To thoroughly investigate how immune cells infiltrate in the microenvironment of PDA, we analyzed the density of multiple immune cells separately in the stromal and tumoral compartments of the PDA tissue.

B cells show a rather low density in the tumor microenvironment. They were homogeneously distributed in the stromal and tumoral compartment with a slight gradient toward the stroma (Figure 1a). Overall, B cells accounted for a small proportion of the cellular immune landscape in the stroma, with a B cell/T cell-ratio of 1:6,1 (mean density of CD20<sup>+</sup> B cells: 115 cells/mm<sup>2</sup>, mean density of CD3<sup>+</sup> T cells: 704

cells/mm<sup>2</sup>). The T cell infiltrate was dominated by CD4<sup>+</sup> T helper cells with a significant spatial proximity to the tumor epithelium (p = .043). On the other hand, CD8<sup>+</sup> cytotoxic T cells were primarily found in the stroma (p < .0001). The same observation was made for CD163<sup>+</sup> tumor-associated macrophages, which significantly assembled in the stromal tissue (p < .0001) (Figure 1a). To assess whether the density of B cells was associated with a specific cytokine signature within the stromal compartment, stroma was classified as “B cell high” or “B cell low” (depending on B cell quantity relative to median B cell number). Focusing on relevant cytokines involved in B cell or TLS functionalities according to previous reports<sup>12–17</sup> (CCL3, CCL4, CXCL9, CXCL10, IL7, IL10, IL17, IFNG, CXCL12, VCAM1 and LTA) no significant differences were found (Figure S1a). The same observation was made for Th1- and Th2-type cytokines<sup>18–20</sup> (Th1 activation: IFNG, TNF, IL2, IL12, IL12B, IL1B; Th2 activation: IL4, IL5, IL9, IL10) (Figure S1b). Also, survival analysis did not reveal a significant prognostic relevance for stromal B cell densities (Figure 1b).

### Formation of TLS and their association with immune phenotypes and patient outcome

The appraisal of B cell distribution in the analyzed tissue specimens called attention to an immune cell clustering in the peritumoral stroma. Systematic stainings revealed the formation of TLS, with a core of CD20<sup>+</sup> B cell agglomerates, few central DC-LAMP<sup>+</sup> dendritic cells, a cluster of CD21<sup>+</sup> follicular dendritic cells and different T cell subtypes (CD3<sup>+</sup>, CD4<sup>+</sup> and CD8<sup>+</sup> T cells shown) (Figure 2a). Also, CD163<sup>+</sup> tumor-associated macrophages were present in TLS; however, their density was higher in the non-TLS stroma (Figure 2a). Interestingly, FoxP3<sup>+</sup> regulatory T cells were absent throughout all observed TLS. TLS were observed in 17 of 55 patient samples (30.9%).

To evaluate the association of TLS with clinical outcomes, we compared the overall survival of patients with “TLS” versus “No TLS” in their PDA specimen. The formation of TLS was significantly associated with an improved patient outcome (p = .018) (Figure 2b). To further assess the association between TLS presence and immune phenotypes, we compared densities of stromal immune cells in “TLS” versus “No TLS” groups. We found that the presence of TLS was associated with significantly higher numbers of stromal CD20<sup>+</sup> B cells (p = .015) and CD8<sup>+</sup> T cells (p = .029) (Figure 2c). No other immune cell type showed a difference in distribution (Figure S2a).

In order to investigate whether TLS associate with distinct cytokine profiles within the peritumoral stroma, we assessed concentrations of stromal Th1- and Th2-type cytokines (Th1 activation: IFNG, TNF, IL2, IL12, IL12B, IL1B; Th2 activation: IL4, IL5, IL9, IL10) in both groups. A prevailing activation state of either Th1 or Th2 cells could not be confined in the stromal compartment of TLS-positive patients (Figure 2d). However, a slight but significant difference was observed in the IL2 concentration, with higher stromal expression in TLS-positive

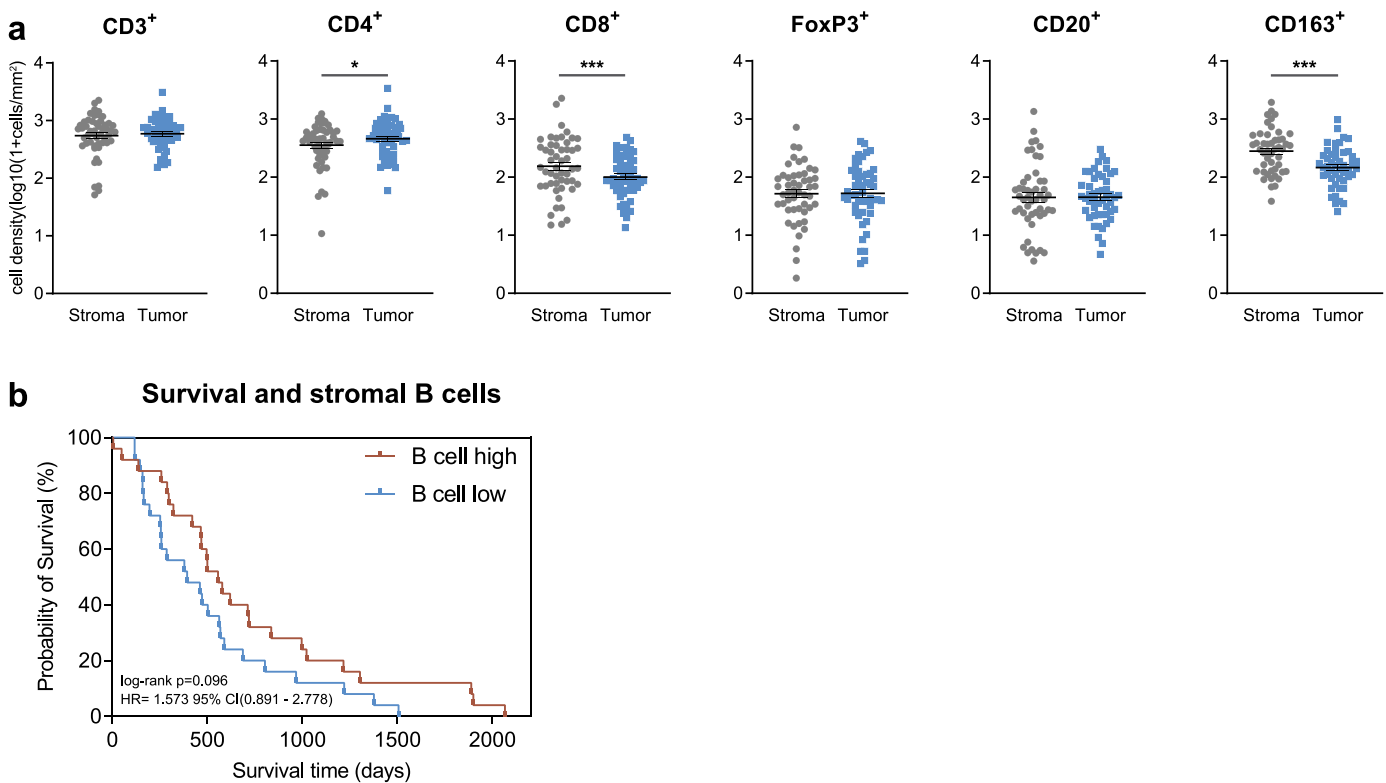


**Figure 1. B cell infiltrate in PDA. (a)** Scatter dot plots comparing the density of immune cells (as indicated) in PDA tissue of patients with stratification in “Tumor” and “Stroma”. Information on immune cell density was available as follows: CD3<sup>+</sup>(n=49), CD4<sup>+</sup>(n=51), CD8<sup>+</sup>(n=51), FoxP3<sup>+</sup>(n=50), CD20<sup>+</sup>(n=50), CD163<sup>+</sup>(n=48). **(b)** Kaplan-Meier survival plot of PDA patients with high versus low stromal B cell density (n=25/n=25). The median cutpoints were determined to stratify patients into high and low. \*p<.05, \*\*\*p<.0001. PDA=Pancreatic ductal adenocarcinoma.

patients ( $p = .008$ ) (Figure 2d). No significant differences were found in cytokines involved in B cell or TLS functionalities (Figures S2b).

Additionally, we evaluated the association of CD21 gene expression with overall survival in PDA patients using data (TCGA Pancreatic Cancer) via the Xena platform.<sup>11</sup> CD21 gene expression was not significantly associated with overall survival ( $p = .286$ ) but showed a tendency toward beneficial patient outcomes (Figure S2c).

### Compartmental IL2 levels and their association with presence of TLS

To further investigate the role of IL2 with regard to the presence of TLS, we performed compartmental analysis to compare the stroma-to-tumor and stroma-to-serum IL2 gradients between patients with and without TLS. Also, we assessed the potential of circulatory IL2 as a predictive biomarker for TLS.

In patients with TLS, we detected a significant stroma-to-tumor IL2 gradient toward the stromal compartment ( $p = .022$ ), while no significant gradient was detected in stromal versus serum IL2 levels (Figure 3a). The opposite observation was made in patients without TLS, in whom a significant stroma-to-serum IL2 gradient toward the serum compartment was found ( $p < .0001$ ) and no differences were detected between the stromal and tumoral compartments (Figure 3a). In serum, low levels of IL2 were significantly associated with

the presence of TLS ( $p = .037$ ). Meanwhile, serum levels of C-reactive protein (CRP), white blood cells (WBC) and CA 19-9 did not relate to the local formation of TLS (Figure 3b).

### Discussion

The recent decade has emphasized the prognostic relevance of the immunological makeup of local microenvironments in solid cancers. In this regard, most of the focus concentrated on the role of T cells, highlighting the association of tumor-infiltrating T lymphocytes with overall patient survival in numerous tumor entities, including PDA.<sup>21–27</sup> Recently, also B cells in context of TLS have been described as critical components of the local immune landscape in terms of patient prognosis and response to immunotherapy.<sup>8,25,28–30</sup> TLS represent an environment with specific dedicated immunomodulatory factors and serve as a site of antigen presentation and T cell activation. However, the full cellular makeup of different organs varies. It can consist of a typically immunogenic microenvironment like in non-small cell lung cancer (NSCLC) or a generally non-immunogenic local landscape of desmoplastic nature in PDA. Consequently, the observed TLS can have different ultrastructures depending on the organ, malignancy or unique microenvironmental conditions. TLS can be highly organized like in NSCLC with exhibition of a structured T cell zone, embedded dendritic cells and B cells and surrounding high endothelial venules.<sup>31–34</sup> TLS in the peritumoral stroma of PDA show similar features, including the presence of CD21<sup>+</sup>



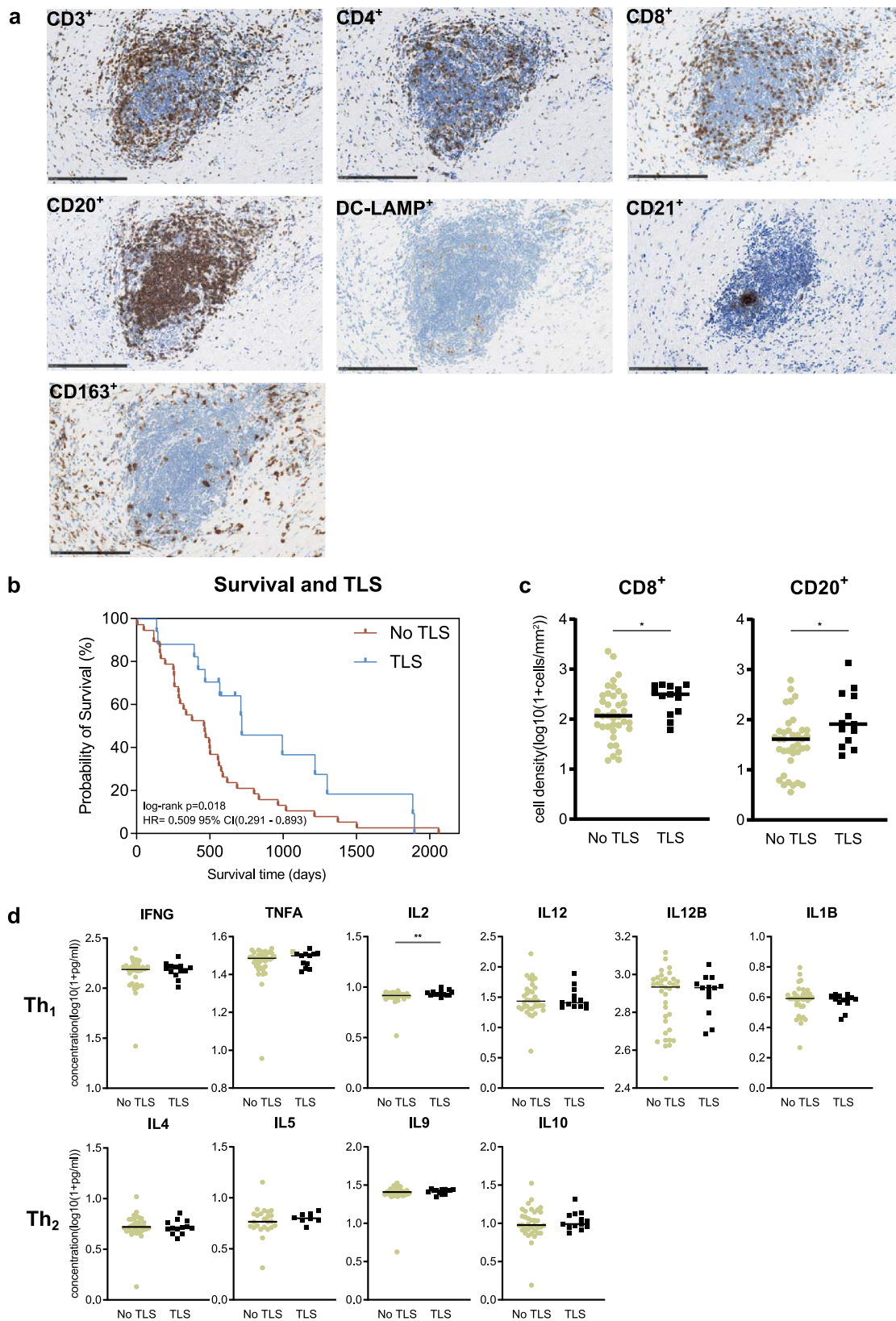


**Figure 2. Formation of TLS and their association with immune phenotypes and patient outcome.** (a) Exemplary detail of TLS in the peritumoral stroma of PDA. Immune cell stainings (as indicated) were all counterstained with H/E. All images: 20x magnification. Scale bar: 250 $\mu$ m. (b) Kaplan-Meier survival plot of PDA patients with "TLS" versus "No TLS" (n=38/n=17). (c) Scatter dot plots comparing the density of CD8<sup>+</sup> T cells and CD20<sup>+</sup> B cells in peritumoral stroma of PDA patients with "TLS" (n = 13) versus "No TLS" (n = 38). (d) Scatter dot plots comparing cytokine concentrations in peritumoral stroma of PDA patients with "TLS" (n = 13) versus "No TLS" (n = 38). Cytokines were categorized in Th1- and Th2-type cytokines (as indicated). \*p  $\leq$  .05, \*\*\*p  $\leq$  .005. TLS = Tertiary lymphoid structures, PDA= Pancreatic ductal adenocarcinoma.

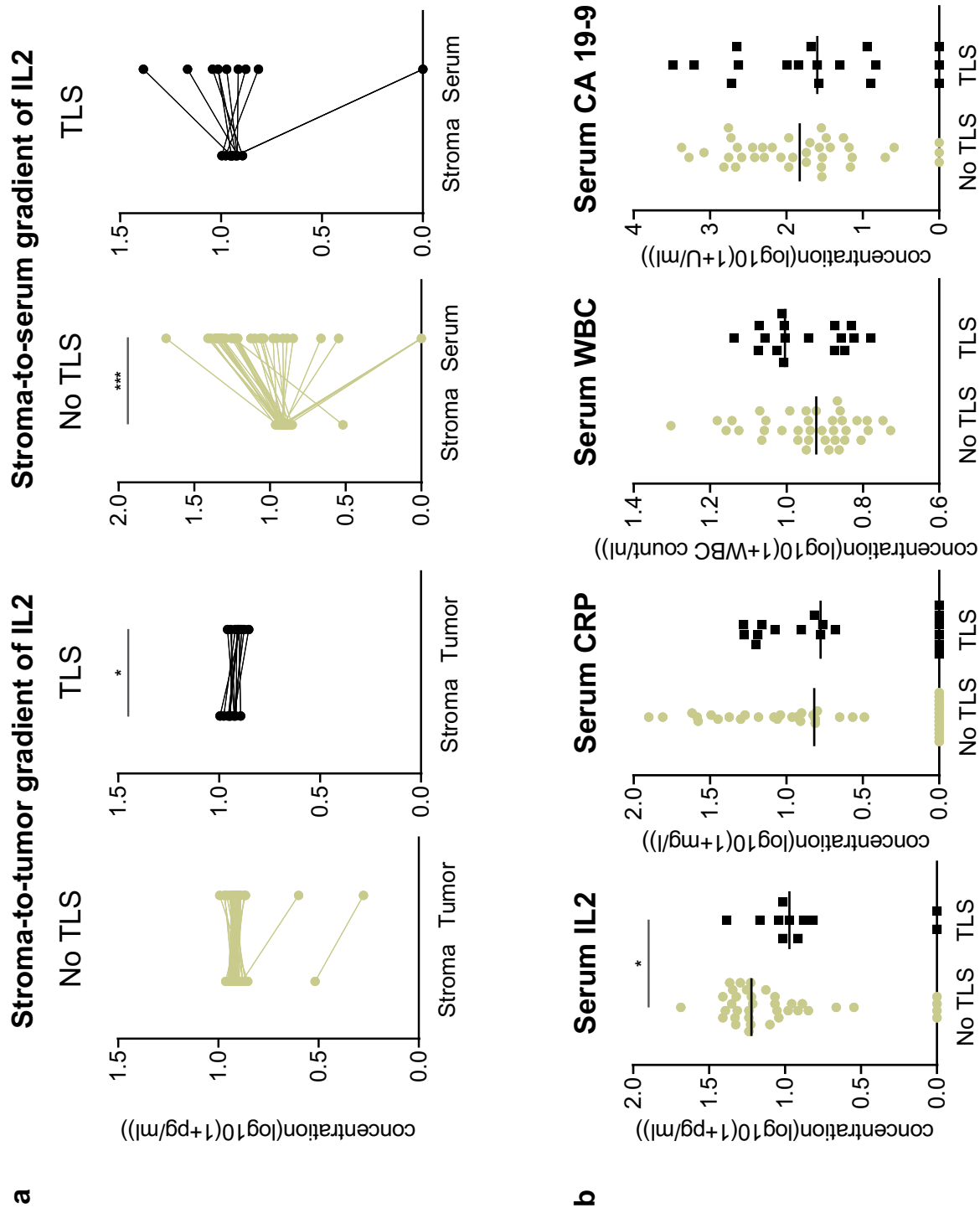


**Figure 3. Compartmental IL2 levels and their association with presence of TLS.** (a) Comparison of PDA patients with "TLS" (n = 13) versus "No TLS" (n = 36) regarding the stroma-to-tumor (left) and stroma-to-serum IL2 gradient (right). (b) Scatter dot plots comparing Serum IL2, Serum CRP, Serum WBC and CA 19-9 concentrations of PDA patients with "TLS" (IL2: n = 13; CRP, WBC, CA 19-9: n = 17) versus "No TLS" (n = 36). \*p ≤ .05, \*\*\*p ≤ .005. TLS = Tertiary lymphoid structures, IL2 = Interleukin-2, CRP = C-reactive protein, WBC = White blood cells, CA 19-9 = Carbohydrate antigen 19-9, PDA = Pancreatic ductal adenocarcinoma.

follicular dendritic cells, but they can also appear as less organized lymphoid aggregates. The dominating presence of CD21<sup>+</sup> follicular dendritic cells within TLS (86% of TLS+ cases) in our analyzed PDA tissues indicates that most peritumoral TLSs in PDA patients are mature. The assessment of the maturation stage of TLSs is important as it has functional implications and differential prognostic relevance in tumors.<sup>35</sup> Such as the association of mature TLS with treatment response to checkpoint inhibition.<sup>36</sup> Another interesting feature of TLS composition that we observe here is the presence of (presumably immunosuppressive) CD163<sup>+</sup> macrophages in PDA. They can potentially undermine antigen presentation and T cell activation in TLS, however, CD163<sup>+</sup> macrophages are known to form lymphoid aggregates upon immunotherapy via vaccination in PDA patients.<sup>37</sup> Despite their presence TLS clearly are a prognostic favorable feature in PDA. So, it is necessary to further understand specific biological features associated with TLS formation in PDA. As discussed above, immunologic programs involved in TLS generation can differ in different tumor types. Further investigation of the role of CD163<sup>+</sup> macrophages for example can help to understand the decisive factors for the specific cancer entity. This can help to better translate relevant findings into the clinic and improve patient care, e.g. by using serum markers as a stratification tool for immunotherapeutic approaches based on local TLS formation. In the past, intratumoral TLS in PDA have been described as favorable prognosticators. However, we corroborate these findings for TLS in the peritumoral stroma and also demonstrate their association to multicompartamental IL2 levels (including matched serum analysis) and present immunological differences between TLS and non-TLS PDA tissues.<sup>5</sup>

A comprehensive assessment of the immune infiltrate considering the compartmental immune cell distribution and cytokine expression patterns revealed that cytotoxic CD8<sup>+</sup> T lymphocytes and tumor-associated CD163<sup>+</sup> macrophages were predominant in the stromal compartment of PDA, which underlines the often described – but debated – immune-excluded nature of PDA.<sup>38</sup> B cells only made a small proportion of the immune infiltrate and did not show a difference in spatial distribution, also their density was not associated with overall survival of patients. However, peritumoral TLS mainly consist of B cells and in line with previous findings formation of TLS proved to be a prognostic favorable marker in our cohort. Further analysis unraveled that PDA tissues with TLS were associated with a higher number of CD8<sup>+</sup> T cells and CD20<sup>+</sup> B cells as well as a higher stromal IL2 concentration when compared to PDA tissues without TLS. This is in line with the observation that TLS-rich tumors usually show higher infiltration by effector CD8<sup>+</sup> T cells which reflects the potential of TLS to activate and differentiate T cells and orchestrate immune responses.<sup>39</sup> In NSCLC, the dendritic cell marker DC-LAMP is associated with Th1 polarization underscoring that T cell education is orchestrated within TLS.<sup>40–42</sup> Moreover, it has been shown that NSCLC with low TLS density identifies patients with poor prognosis within the cohort with high CD8<sup>+</sup> T cell counts, pointing toward a functional heterogeneity among the CD8<sup>+</sup> T cells.<sup>40</sup> This implies that education of T cells in TLS is important to exhibit antitumoral effects. Therefore, it

fits well that high densities of both CD8<sup>+</sup> and CD20<sup>+</sup> lymphocytes are related to prognostic favorable TLS presence in our cohort. The density of B cells alone is not relevant in terms of patient prognosis, and one could hypothesize that T cell density alone only partially reflects the full picture as their functional status (e.g. activation) is not easily assessable and therefore not investigated regularly. The other factor related to TLS presence in our cohort was IL2. Under steady-state conditions IL2 is primarily produced by activated CD4<sup>+</sup> T cells in secondary lymphoid organs. During an immune response, activated CD4<sup>+</sup> and CD8<sup>+</sup> T lymphocytes secrete large quantities of IL2 and duration of the IL2 signal controls the expansion of antigen-specific CD8<sup>+</sup> T cell populations. In malignancies, IL2 exhibits a variety of antitumoral functions including the promotion of a Th1 phenotype leading to proliferation and activation of cytotoxic T cells.<sup>43</sup> We wondered whether compartmental evaluation of IL2 levels could shed further light on the role of IL2 with regard to TLS formation. In PDA tissues with TLS, higher IL2 levels were found in the stromal than in the tumoral compartment whereas no difference was detected in tissues without TLS. This is indicative of an antitumoral environment related to TLS presence or formation in the peritumoral stroma and could explain the higher CD8<sup>+</sup> T cell density in the stroma of PDA tissues with TLS. This observation underlines that knowledge of compartmentalization of a given cytokine is important to better assess biological features of a TME, especially since evaluation of gradients formed by cytokines are a prerequisite to comprehend their functionality.<sup>44</sup> In our study, IL2 compartmentalization in TLS fundamentally differed from non-TLS PDA specimens. Focusing on the stroma-to-serum gradient, patients without TLS showed higher IL2 levels in circulation than in the stromal compartment, while no such gradient was found in patients with TLS. Additionally, low circulatory IL2 concentration was associated with existence of TLS. These findings propose that circulatory IL2 is a potential candidate for further biomarker studies. Besides, high serum IL2 levels can also be measured during inflammatory states. However, the classical inflammatory markers CRP and WBC in patients without TLS did not indicate such a state in our cohort and indicate a differential regulatory inflammatory state.

TLS are likely to have an impact on immunotherapeutic strategies in the future. Open questions include the relation of TLS to treatment successes for chemotherapy, radiation or other interventions.<sup>45–47</sup> Current preclinical approaches focus on strategies aiming to induce TLS neogenesis in tumors. This could improve anti-tumor immunity and possibly allow to turn immune-low into immune-high tumors in combination with immunotherapies such as immune checkpoint inhibition.<sup>6,12,48,49</sup> Approaches for specific induction of TLS are being investigated using cytokines, stromal cells, antigen-presenting cells, antibodies, inflammatory factors or other agents.<sup>6,50–55</sup> However, so far, the main translatory potential of TLS lies in their ability to predict positive immunotherapy responses in various tumor entities. Accessibility to tissue samples is especially demanding in PDA, also due to the invasive nature of tissue acquisition and complications. Therefore, identification of easily

accessible and reliable surrogate markers for TLS formation is an unmet need when it comes to clinical practice. With serum IL2, we have now identified a cytokine of interest in this regard. However, this needs to be independently validated in prospective trials, also focusing on other factors influencing the serum IL2 levels in patients and in order to define applicable threshold values.

Overall, the results of our study underscore the prognostic role of TLS in the peritumoral stroma of PDA and indicate their potential to shape local antitumoral properties by being associated with higher densities of cytotoxic T cells in the TME. Also, we highlight the complex interaction of TLS with multi-compartmental IL2 expression, proposing circulatory IL2 levels as markers for TLS presence in the tumor micro-environment. As an outlook, the link between IL2 and TLS formation can be exploited clinically by e.g. improving patient stratification for immunotherapeutic strategies. We propose that circulatory IL2 levels should be regularly assessed in clinical studies which investigate TLS formation in malignancies. Their predictive potential for local TLS formation could possibly also be applied to other entities. Also, we highlight the importance of compartmental evaluation of biological features of tumors to better understand dynamics of antitumoral immune responses.

## Acknowledgments

We thank Jana Wolf, Ulrike Prüfer and Rosa Eurich for excellent technical assistance. PDA samples were provided by the Pancobank platform at the European Pancreas Center Heidelberg (EPZ), member of the Biomaterial Bank Heidelberg (BMBH). The results published here are in part based upon data generated by the TCGA Research Network: <https://www.cancer.gov/tcga>.

## Disclosure statement

No potential conflict of interest was reported by the author(s).

## Funding

This work was supported by the RR Pohl Stiftung.

## ORCID

Azaz Ahmed  <http://orcid.org/0000-0003-3000-7951>  
Niels Halama  <http://orcid.org/0000-0003-0344-6027>

## Data availability statement

All data are available upon request. All data relevant to the study are included in the article.

## Author's contributions

Conceptualization, A.A., S. K. and N.H.; Methodology, A.A., S.K. and N. H.; Formal Analysis, A.A. and N.H.; Investigation, A.A., S.K. and R.K.; Resources, R.K., T.H., N.G., C.S., I.Z., D.J. and N.H.; Data Curation, A. A. and N.H.; Writing—Original Draft, A.A.; Writing—Review & Editing, A.A., R.K., S.K., N.G., C.S., I.Z., D.J. and N.H.; Visualization, A.A. and N. H.; Supervision, I.Z., D.J. and N.H.; Project Administration, A.A. and N. H.; Funding Acquisition, I.Z., D.J. and N.H.

## References

- Karamitopoulou E. Tumour microenvironment of pancreatic cancer: immune landscape is dictated by molecular and histopathological features. *Br J Cancer*. 2019;121(1):5–14. doi:10.1038/s41416-019-0479-5.
- Pylayeva-Gupta Y, Das S, Handler JS, Hadju CH, Coffre M, Koralov SB, Bar-Sagi D. IL35-producing B cells promote the development of pancreatic neoplasia. *Cancer Discov*. 2016;6(3):247–255. doi:10.1158/2159-8290.CD-15-0843.
- Lee KE, Spata M, Bayne LJ, Buza EL, Durham AC, Allman D, Vonderheide RH, Simon MC. Hif1a deletion reveals pro-neoplastic function of B cells in pancreatic neoplasia. *Cancer Discov*. 2016;6(3):256–269. doi:10.1158/2159-8290.CD-15-0822.
- Roghani A, Fraser C, Kleyman M, Chen J. B cells promote pancreatic tumorigenesis. *Cancer Discov*. 2016;6(3):230–232. doi:10.1158/2159-8290.CD-16-0100.
- Hiraoka N, Ino Y, Yamazaki-Itoh R, Kanai Y, Kosuge T, Shimada K. Intratumoral tertiary lymphoid organ is a favourable prognosticator in patients with pancreatic cancer. *Br J Cancer*. 2015;112(11):1782–1790. doi:10.1038/bjc.2015.145.
- Sautès-Fridman C, Petitprez F, Calderaro J, Fridman WH. Tertiary lymphoid structures in the era of cancer immunotherapy. *Nat Rev Cancer*. 2019;19(6):307–325. doi:10.1038/s41568-019-0144-6.
- Dieu-Nosjean M-C, Goc J, Giraldo NA, Sautès-Fridman C, Fridman WH. Tertiary lymphoid structures in cancer and beyond. *Trends Immunol*. 2014;35(11):571–580. doi:10.1016/j.it.2014.09.006.
- Helms BA, Reddy SM, Gao J, Zhang S, Basar R, Thakur R, Yizhak K, Sade-Feldman M, Blando J, Han G, et al. B cells and tertiary lymphoid structures promote immunotherapy response. *Nature*. 2020;577(7791):549–555. doi:10.1038/s41586-019-1922-8.
- Edge SB, Compton CC. The American Joint committee on cancer: the 7th edition of the AJCC cancer staging manual and the future of TNM. *Ann Surg Oncol*. 2010;17(6):1471–1474. doi:10.1245/s10434-010-0985-4.
- Halama N, Zoernig I, Berthel A, Kahlert C, Klupp F, Suarez-Carmona M, Suetterlin T, Brand K, Krauss J, Lasitschka F, et al. Tumoral immune cell exploitation in colorectal cancer metastases can be targeted effectively by anti-CCR5 therapy in cancer patients. *Cancer Cell*. 2016;29(4):587–601. doi:10.1016/j.ccell.2016.03.005.
- Goldman MJ, Craft B, Hastie M, Repečka K, McDade F, Kamath A, Banerjee A, Luo Y, Rogers D, Brooks AN, et al. Visualizing and interpreting cancer genomics data via the Xena platform. *Nat Biotechnol*. 2020;38(6):675–678. doi:10.1038/s41587-020-0546-8.
- Zhu G, Falahat R, Wang K, Mailloux A, Artzi N, Mulé JJ. Tumor-associated tertiary lymphoid structures: gene-expression profiling and their bioengineering. *Front Immunol*. 2017;8:767. doi:10.3389/fimmu.2017.00767.
- Fu Y-X, Chaplin DD. Development and maturation of secondary lymphoid tissues. *Annu Rev Immunol*. 1999;17(1):399–433. doi:10.1146/annurev.immunol.17.1.399.
- Luther SA, Bidgol A, Hargreaves DC, Schmidt A, Xu Y, Paniyadi J, Matloubian M, Cyster JG. Differing activities of homeostatic chemokines CCL19, CCL21, and CXCL12 in lymphocyte and dendritic cell recruitment and lymphoid neogenesis. *J Immunol*. 2002;169(1):424–433. doi:10.4049/jimmunol.169.1.424.
- Jacquelot N, Tellier J, Nutt SL, BG. Tertiary lymphoid structures and B lymphocytes in cancer prognosis and response to immunotherapies. *Oncoimmunology*. 2021;10:(1).
- Cai C, Zhang J, Li M, Wu Z-J, Song KH, Zhan TW, Wang L-H, Sun Y-H. Interleukin 10-expressing B cells inhibit tumor-infiltrating T cell function and correlate with T cell Tim-3 expression in renal cell carcinoma. *Tumor Biology*. 2016;37(6):8209–8218. doi:10.1007/s13277-015-4687-1.



17. Tang H, Zhu M, Qiao J, Fu Y-X. Lymphotoxin signalling in tertiary lymphoid structures and immunotherapy. *Cell Mol Immunol.* 2017;14(10):809–818. doi:10.1038/cmi.2017.13.
18. Zhou L, Chong MM, Littman DR. Plasticity of CD4+ T cell lineage differentiation. *Immunity.* 2009;30(5):646–655. doi:10.1016/j.immuni.2009.05.001.
19. Lee HL, Da Rocha GO, de Andrade JB. Inflammatory cytokines and change of Th1/Th2 balance as prognostic indicators for hepatocellular carcinoma in patients treated with transarterial chemoembolization. *Sci Rep.* 2019;9(1):1–8. doi:10.1038/s41598-018-37186-2.
20. Paul WE, Seder RA. Lymphocyte responses and cytokines. *Cell.* 1994;76(2):241–251. doi:10.1016/0092-8674(94)90332-8.
21. Fridman WH, Zitvogel L, Sautès-Fridman C, Kroemer G. The immune contexture in cancer prognosis and treatment. *Nat Rev Clin Oncol.* 2017;14(12):717–734. doi:10.1038/nrclinonc.2017.101.
22. Carstens JL, Correa de Sampaio P, Yang D, Barua S, Wang H, Rao A, Allison JP, LeBleu VS, Kalluri R. Spatial computation of intratumoral T cells correlates with survival of patients with pancreatic cancer. *Nat Commun.* 2017;8(1):1–13. doi:10.1038/ncomms15095.
23. Balachandran VP, Łuksza M, Zhao JN, Makarov V, Moral JA, Remark R, Herbst B, Askan G, Bhanot U, Senbabaoğlu Y, et al. Identification of unique neoantigen qualities in long-term survivors of pancreatic cancer. *Nature.* 2017;551(7681):512–516. doi:10.1038/nature24462.
24. Sautès-Fridman C, Lawand M, Giraldo NA, Kaplon H, Germain C, Fridman WH, Dieu-Nosjean M-C. Tertiary lymphoid structures in cancers: prognostic value, regulation, and manipulation for therapeutic intervention. *Front Immunol.* 2016;7:407. doi:10.3389/fimmu.2016.00407.
25. Germain C, Gnjjatic S, Tamzali F, Knockaert S, Remark R, Goc J, Lepelley A, Becht E, Katsahian S, Bizouard G, et al. Presence of B cells in tertiary lymphoid structures is associated with a protective immunity in patients with lung cancer. *Am J Respir Crit Care Med.* 2014;189(7):832–844. doi:10.1164/rccm.201309-1611OC.
26. Rouanne M, Arpaia N, Marabelle A. CXCL13 shapes tertiary lymphoid structures and promotes response to immunotherapy in bladder cancer. *Eur J Cancer.* 2021;151:245–248. doi:10.1016/j.ejca.2021.03.054.
27. Wirsing AM, Rikardsen OG, Steigen SE, Uhlin-Hansen L, Hadler-Olsen E. Characterisation and prognostic value of tertiary lymphoid structures in oral squamous cell carcinoma. *BMC Clin Pathol.* 2014;14(1):1–10. doi:10.1186/1472-6890-14-38.
28. Cabrita R, Lauss M, Sanna A, Donia M, Skaarup Larsen M, Mitra S, Johansson I, Phung B, Harbst K, Vallon-Christersson J, et al. Tertiary lymphoid structures improve immunotherapy and survival in melanoma. *Nature.* 2020;577(7791):561–565. doi:10.1038/s41586-019-1914-8.
29. Petitprez F, de Reyniès A, Keung EZ, Chen TWW, Sun C-M, Calderaro J, Jeng Y-M, Hsiao L-P, Lacroix L, Bougouin A, et al. B cells are associated with survival and immunotherapy response in sarcoma. *Nature.* 2020;577(7791):556–560. doi:10.1038/s41586-019-1906-8.
30. Thommen DS, Koelzer VH, Herzig P, Roller A, Trefny M, Dimeloe S, Kiiälainen A, Hanhart J, Schill C, Hess C, et al. A transcriptionally and functionally distinct PD-1+ CD8+ T cell pool with predictive potential in non-small-cell lung cancer treated with PD-1 blockade. *Nat Med.* 2018;24(7):994–1004. doi:10.1038/s41591-018-0057-z.
31. de Chaisemartin L, Goc J, Damotte D, Validire P, Magdeleinat P, Alifano M, Cremer I, Fridman W-H, Sautès-Fridman C, Dieu-Nosjean M-C, et al. Characterization of chemokines and adhesion molecules associated with T cell presence in tertiary lymphoid structures in human lung cancer. *Cancer Res.* 2011;71(20):6391–6399. doi:10.1158/0008-5472.CAN-11-0952.
32. Martinet L, Garrido I, Filleron T, Le Guellec S, Bellard E, Fournie -J-J, Rochaix P, Girard J-P. Human solid tumors contain high endothelial venules: association with T- and B-lymphocyte infiltration and favorable prognosis in breast cancer. *Cancer Res.* 2011;71(17):5678–5687. doi:10.1158/0008-5472.CAN-11-0431.
33. Dieu-Nosjean MC, Giraldo NA, Kaplon H, Germain C, Fridman WH, Sautès-Fridman C. Tertiary lymphoid structures, drivers of the anti-tumor responses in human cancers. *Immunol Rev.* 2016;271(1):260–275. doi:10.1111/imr.12405.
34. Munoz-Eraza L, Rhodes JL, Marion VC, Kemp RA. Tertiary lymphoid structures in cancer—considerations for patient prognosis. *Cell Mol Immunol.* 2020;17(6):570–575. doi:10.1038/s41423-020-0457-0.
35. Dai S, Zeng H, Liu Z, Jin K, Jiang W, Wang Z, Lin Z, Xiong Y, Wang J, Chang Y, et al. Intratumoral CXCL13+CD8+T cell infiltration determines poor clinical outcomes and immunoevasive contexture in patients with clear cell renal cell carcinoma. *J Immuno Cancer.* 2021;9(2):e001823. doi:10.1136/jitc-2020-001823.
36. Vanhersecke L, Brunet M, Guégan J-P, Rey C, Bougouin A, Cousin S, Le Moulec S, Besse B, Loriot Y, Larroquette M, et al. Mature tertiary lymphoid structures predict immune checkpoint inhibitor efficacy in solid tumors independently of PD-L1 expression. *Nature Cancer.* 2021;2(8):794–802. doi:10.1038/s43018-021-00232-6.
37. Lutz ER, Wu AA, Bigelow E, Sharma R, Mo G, Soares K, Solt S, Dorman A, Wamwea A, Yager A, et al. Immunotherapy converts nonimmunogenic pancreatic tumors into immunogenic foci of immune regulation. *Cancer Immuno Res.* 2014;2(7):616–631. doi:10.1158/2326-6066.CIR-14-0027.
38. Sharma P, Allison JP. The future of immune checkpoint therapy. *Science.* 2015;348(6230):56–61. doi:10.1126/science.aaa8172.
39. Sautès-Fridman C, Verneau J, Sun C, Moreira M, Chen TW, Meylan M, Petitprez F, and Fridman WH. Tertiary lymphoid structures and B cells: clinical impact and therapeutic modulation in cancer. *Sem Immunol.* 2020;48:101406. doi:10.1016/j.smim.2020.101406.
40. Goc J, Germain C, Vo-Bourgais TKD, Lupo A, Klein C, Knockaert S, de Chaisemartin L, Ouakrim H, Becht E, Alifano M, et al. Dendritic cells in tumor-associated tertiary lymphoid structures signal a Th1 cytotoxic immune contexture and license the positive prognostic value of infiltrating CD8+T cells. *Cancer Res.* 2014;74(3):705–715. doi:10.1158/0008-5472.CAN-13-1342.
41. Dieu-Nosjean M-C, Antoine M, Danel C, Heudes D, Wislez M, Poulot V, Rabbe N, Laurans L, Tartour E, de Chaisemartin L, et al. Long-term survival for patients with non-small-cell lung cancer with intratumoral lymphoid structures. *J Clin Oncol.* 2008;26(27):4410–4417. doi:10.1200/JCO.2007.15.0284.
42. Lin L, Hu X, Zhang H, Hu H. Tertiary lymphoid organs in cancer immunology: mechanisms and the new strategy for immunotherapy. *Front Immunol.* 2019;10:1398. doi:10.3389/fimmu.2019.01398.
43. Ross SH, Cantrell DA. Signaling and function of inter leukin-2 in T lymphocytes. *Annu Rev Immunol.* 2018;36:411–433.
44. Ahmed A, Köhler S, Klotz R, Giese N, Lasitschka F, Hackert T, Springfield C, Zörnig I, Jäger D, Halama N, et al. Peripheral blood and tissue assessment highlights differential tumor-circulatory gradients of IL2 and MIF with prognostic significance in resectable pancreatic ductal adenocarcinoma. *OncoImmunology.* 2021;10(1):1962135. doi:10.1080/2162402X.2021.1962135.
45. Delvecchio FR, Fincham REA, Spear S, Clear A, Roy-Luzarraga M, Balkwill FR, Gribben JG, Bombardieri M, Hodivala-Dilke K, Capasso M, et al. Pancreatic cancer chemotherapy is potentiated

- by induction of tertiary lymphoid structures in mice. *Cell Mol Gastroenterol Hepatol.* 2021;12(5):1543–1565. doi:10.1016/j.jcmgh.2021.06.023.
46. Boivin G, Kalambaden P, Faget J, Rusakiewicz S, Montay-Gruel P, Meylan E, Bourhis J, Lesec G, Vozenin M-C. Cellular composition and contribution of tertiary lymphoid structures to tumor immune infiltration and modulation by radiation therapy. *Front Oncol.* 2018;8:256. doi:10.3389/fonc.2018.00256.
  47. Morcrette G, Hirsch TZ, Badour E, Pilet J, Caruso S, Calderaro J, Martin Y, Imbeaud S, Letouzé E, Rebouissou S, et al. APCgermline hepatoblastomas demonstrate cisplatin-induced intratumor tertiary lymphoid structures. *Oncoimmunology.* 2019;8(6):e1583547. doi:10.1080/2162402X.2019.1583547.
  48. Weiden J, Tel J, Figdor CG. Synthetic immune niches for cancer immunotherapy. *Nat Rev Immunol.* 2018;18(3):212–219. doi:10.1038/nri.2017.89.
  49. Rodriguez AB, Engelhard VH. Insights into tumor-associated tertiary lymphoid structures: novel targets for antitumor immunity and cancer immunotherapy: tertiary lymphoid structures in cancer. *Cancer Immuno Res.* 2020;8(11):1338. doi:10.1158/2326-6066.CIR-20-0432.
  50. Zhu G, Nemoto S, Mailloux AW, Perez-Villaruel P, Nakagawa R, Falahat R, Berglund AE, Mulé JJ. Induction of tertiary lymphoid structures with antitumor function by a lymph node-derived stromal cell line. *Front Immunol.* 2018;9:1609. doi:10.3389/fimmu.2018.01609.
  51. Chen L, Taylor JL, Sabins NC, Lowe DB, Qu Y, You Z, Storkus WJ. Extranodal induction of therapeutic immunity in the tumor microenvironment after intratumoral delivery of Tbet gene-modified dendritic cells. *Cancer Gene Ther.* 2013;20(8):469–477. doi:10.1038/cgt.2013.42.
  52. Weinstein AM, Chen L, Brzana EA, Patil PR, Taylor JL, Fabian KL, Wallace CT, Jones SD, Watkins SC, Lu B, et al. Tbet and IL-36y cooperate in therapeutic DC-mediated promotion of ectopic lymphoid organogenesis in the tumor microenvironment. *Oncoimmunology.* 2017;6(6):e1322238. doi:10.1080/2162402X.2017.1322238.
  53. Yang S-C, Batra RK, Hillinger S, Reckamp KL, Strieter RM, Dubinett SM, Sharma S. Intrapulmonary administration of CCL21 gene-modified dendritic cells reduces tumor burden in spontaneous murine bronchoalveolar cell carcinoma. *Cancer Res.* 2006;66(6):3205–3213. doi:10.1158/0008-5472.CAN-05-3619.
  54. Aoyama S, Nakagawa R, Mulé JJ, Mailloux AW. Inducible tertiary lymphoid structures: promise and challenges for translating a new class of immunotherapy. *Front Immunol.* 2021;12:1766. doi:10.3389/fimmu.2021.675538.
  55. Johansson-Percival A, He B, Li Z-J, Kjellén A, Russell K, Li J, Larma I, Ganss R. De novo induction of intratumoral lymphoid structures and vessel normalization enhances immunotherapy in resistant tumors. *Nat Immunol.* 2017;18(11):1207–1217. doi:10.1038/ni.3836.